



## Losses and Efficiency Calculation for Multi-Port Converter

Downloaded from: <https://research.chalmers.se>, 2024-05-02 22:42 UTC

Citation for the original published paper (version of record):

Anuradha, C., Vijayalakshmi, S., Ganesh, V. et al (2022). Losses and Efficiency Calculation for Multi-Port Converter. AIP Conference Proceedings, 2516. <http://dx.doi.org/10.1063/5.0108657>

N.B. When citing this work, cite the original published paper.

# Losses and efficiency calculation for multi-port converter

Cite as: AIP Conference Proceedings **2516**, 140002 (2022); <https://doi.org/10.1063/5.0108657>  
Published Online: 30 November 2022

C. Anuradha, S. Vijayalakshmi, Viswanathan Ganesh, et al.



View Online



Export Citation

## ARTICLES YOU MAY BE INTERESTED IN

[A comprehensive review on LoRa implementation in IoT application domains](#)

AIP Conference Proceedings **2516**, 140001 (2022); <https://doi.org/10.1063/5.0108994>

[Brushless DC motor force ripple reduction techniques - A survey](#)

AIP Conference Proceedings **2516**, 140004 (2022); <https://doi.org/10.1063/5.0109582>

[Factor analysis for spread of HIV in a mobile heterosexual population](#)

AIP Conference Proceedings **2516**, 130007 (2022); <https://doi.org/10.1063/5.0108789>



## APL Quantum

**CALL FOR APPLICANTS**

### Seeking Editor-in-Chief

# Losses and Efficiency Calculation for Multi-Port Converter

C.Anuradha<sup>1,a)</sup>, S.Vijayalakshmi<sup>1,b)</sup>, Viswanathan Ganesh<sup>2,c)</sup>, Venkata Subramani<sup>1,d)</sup>

<sup>1</sup> Department of Electrical & Electronics Engineering, SRMIST, Kattankolathur, Tamilnadu, India, Pincode-603203.

<sup>2</sup> Department of Electrical Engineering, Chalmers University of Technology, SE-412 96 Gothenburg, Sweden.

<sup>a)</sup> Corresponding author: anuradh@srmist.edu.in,

<sup>b)</sup> vijayals@srmist.edu.in, <sup>c)</sup> viswanathanganesh1999@gmail.com,

<sup>d)</sup> venkatasubramani69@gmail.com.

**Abstract:** In this paper, a multi-port non-isolated SEPIC converter is analysed for integrating with the renewable energy source and also losses and efficiency are calculated. The proposed converter utilizes a single stage power conversion, thereby providing higher energy efficiency. The proposed structure comprises of a combination of Pulsating Voltage Cells (PVC) and Pulsating Voltage Source Cell (PVSC) on the input side and a Pulsating Voltage Load Cell (PVLC) on the output side. The two topologies involved are Multi Input Single Output (MISO) and Multi Input Multiple Output (MIMO) which are bidirectional. The efficiency of the proposed multi-port converter has been calculated by determining the switching stress of the power electronic switches used. The proposed multi-port SEPIC converter considers the entire system to be a single-stage converter, and promises higher energy efficiency.

## INTRODUCTION

The recent trend sees an ever-expanding market for renewable energy based power generation to serve as a viable replacement for conventional fossil fuel based power generation. Such power systems need to be interfaced in a proper manner to efficiently handle various energy sources. With multiple inputs of power supply we could combine their advantages, increase the reliability of the system and effectively utilize the energy sources. Conventional multi-input power converter (MIPC) consists of multiple sources fed through separate converters that make the structure Complex and control technique difficult. Because of this reason the implementation effort of MIPC is high. [1-5]. The Fig.1 shows conventional Multi-input converter diagram.

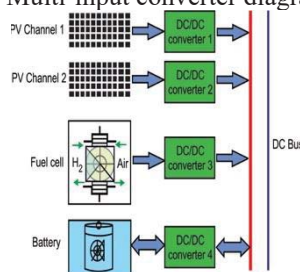


FIGURE 1. - Conventional Multi-input converter

To overcome these difficulties in MIPC, Multi Port Converter (MPC) is of potential interest in generation systems utilizing multiple renewable energy sources. In MPCs, multiple sources are fed to the load by a single stage modified DC/DC converter. This leads to reduce the complexity the structure as well as the control technique. [6]

MPCs are basically classified into four categories as follows:

1. Based on topology (series and parallel)
2. Based on port placement (SISO, MISO and MIMO)
3. Based on coupling (isolated and non-isolated)

4. Based on conversion process (unidirectional and bidirectional). [7-8]

## SELECTION OF CONVERTER MODEL

By connection of sources in series there is certain problems like-

- The current of the entire string is limited by the weakest current.
- Voltage-sagging results in excessive demand on converter designs.

To overcome these problems, parallel-connected topologies are employed.

As renewable energy sources are intermittent in nature, usage of storage devices is necessary to improve reliability of the system. Bidirectional MPC consists of bidirectional ports that can be utilized for connecting storage devices. Isolated MPCs are derived with the help of magnetic coupling (through multi winding transformers). These MPCs are sensible in case of applications involving isolation and bidirectional conversion. The major disadvantage is presence of transformer and large number of active switches that result in a bulky structure. So we opt for a Non-Isolated structure that does not use transformer and gives us a simple and economic structure. [9-12]. The Fig.2 shows proposed Multi port structure diagram.

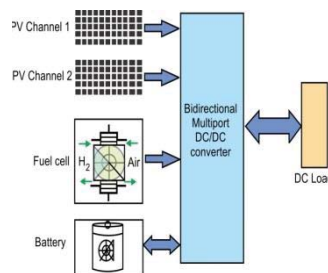


FIGURE 2. - Proposed Multi port structure

DC-DC converters are usually used to vary the input voltage or change its polarity. A DC/DC converter operates by rapidly switching on and switching off a switch. There are different types of DC/DC converters that can be used for the implementation of multiport structure. [13-15]

Some of them are Buck converter, Boost converter, Buck-Boost converter, Cuk converter, SEPIC etc. In this project the proposed structure is a parallel connected non-isolated SEPIC/SEPIC bidirectional MPC. [16-17]

Advantages of Proposed Converter model:

- In SEPIC converter the input current is continuous unlike in buck-boost converter thus SEPIC converter has better power factor than buck-boost converter
- SEPIC converter has a non-inverting output which is not available in Cuk converter and Buck-boost converter.
- In SEPIC converter a capacitor is connected in series for coupling the energy between input and output. So when the switch is turned off, its output comes down to 0V.
- The proposed converter can be used in applications that require separate voltage levels with bidirectional current path.
- The possibility of using different energy sources with different voltage-current characteristics, lower cost, continuous input current, and transformer-less output are the major advantages of the converter.

## SEPIC CONVERTER

The SEPIC converter is one of the first generation developed DC/DC converter that allows the output voltage to be more, less or equal to its source voltage. Fig.3 shows the Schematic of SEPIC converter.

## Working of Sepic Converter

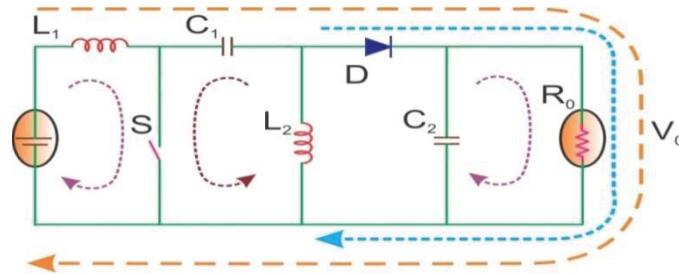


**FIGURE 3.** - Schematic of SEPIC

The structure of SEPIC converter is illustrated in Figure 3. It is a fourth order converter that consists two inductors ( $L_1$  and  $L_2$ ), two capacitors ( $C_1$  and  $C_2$ ), an active switch  $S$  and a diode  $D$ .

The features of SEPIC topology over other topologies are listed:

- Steps up/down its input voltage.
- Produces non-inverted voltage output.
- Low input current ripple due to the input inductor.
- Enhanced efficiency and higher voltage transfer ratio.

The duty ratio controls the semiconductor switch in the SEPIC converter and regulates the output voltage. A series capacitor is an energy buffer which transfers source power to the load.

Turning ON the switch it makes the total input voltage to be appearing across the inductor  $L_1$ . Hence, the inductor current  $I_{L1}$  increases linearly. The buffer capacitor  $C_1$  is assumed to be pre-charged. It discharges and magnetizes the inductor  $L_2$ . Therefore, the inductor current  $I_{L2}$  increases linearly. Meanwhile, the load is maintained by the capacitor  $C_2$ .

During this state, both the voltage source and the inductor transfer their energies to the capacitor  $C_1$  and load as illustrated in Figure 3. The current flows in the path  $L_1$ - $C_1$ - $D$ - $C_2$ & $R$ - $V$ . Also, the inductor  $L_2$  starts demagnetizing and supplies power to load through diode  $D_1$ .

## PROPOSED BI-DIRECTIONAL THREE PORT TOPOLOGY

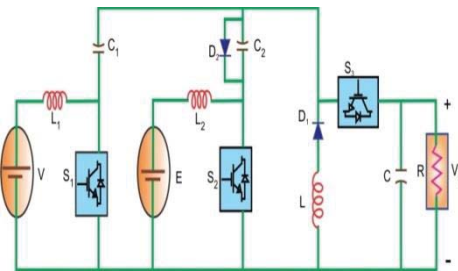


**FIGURE 4.** Proposed Bi-directional three port SEPIC Converter

### Modes of Operation

*Mode-1:  $S_1$  ON,  $S_2$  OFF ( $D$ )*

The equivalent circuit configuration of the proposed Bi-directional three port SEPIC Converter during this mode have been presented in Figure 5. In this state,  $S_1$  is turned ON for the duty cycle  $D$ , But,  $S_2$  and  $S_3$  are not conducting. The energy stored in the capacitor  $C_1$  is released to charge capacitor  $C_2$  through switch  $S_1$  and antiparallel diode of  $S_2$ . Also, capacitor  $C_1$  magnetizes the output inductor  $L$ . The energy stored in  $L_2$  freewheels through the battery and charges it. The source ( $V$ ) magnetizes the inductor  $L_1$ . The positive voltage appearing on inductors, linearly increases their currents. Because of the reverse voltage on the anti-parallel diode of  $S_3$ , it is not conducting. Hence, the capacitor  $C$  caters power to the load.

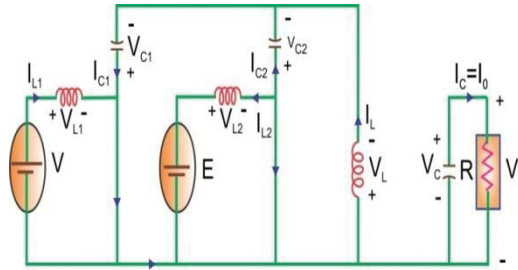


FIGURE 5. - Mode-1: S<sub>1</sub> ON, S<sub>2</sub> OFF

Mode-2: S<sub>1</sub> OFF, S<sub>2</sub> OFF (1-D)

All the switches S<sub>1</sub>, S<sub>2</sub> and S<sub>3</sub> are OFF. The equivalent circuit of this state is depicted in Figure 6. The source V at port-1 together with stored energy inductor L<sub>1</sub> charge the capacitor C<sub>1</sub>. Since S<sub>2</sub> is OFF, the capacitor C<sub>2</sub> discharges and charges the battery through the inductor L<sub>2</sub>. Due to this L<sub>2</sub> stores energy. The source V along with the output inductor supplies power to load through the anti-parallel diode of S<sub>3</sub>.

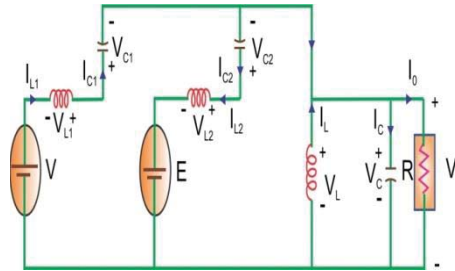


FIGURE 6. - Mode-2: S<sub>1</sub> OFF, S<sub>2</sub> OFF

## STEADY STATE ANALYSIS OF THREE PORT TOPOLOGY

Both the modes of operations are considered to be in CCM. The steady state equations of each mode are given below:

Mode-1: S<sub>1</sub> ON, S<sub>2</sub> OFF (D)

$$L_1 \frac{di_{L1}}{dt} = V \quad (1)$$

$$L_2 \frac{di_{L2}}{dt} = -E \quad (2)$$

$$L \frac{di_L}{dt} = V_{C1} \quad (3)$$

$$C_1 \frac{dV_{C1}}{dt} = C_2 \frac{dV_{C2}}{dt} + i_L \quad (4)$$

$$C \frac{dV_C}{dt} = -\frac{V_C}{R} \quad (5)$$

Mode-2: S<sub>1</sub> OFF, S<sub>2</sub> OFF (1-D)

$$L_1 \frac{di_{L1}}{dt} = V - V_{C1} - V_C \quad (6)$$

$$L_2 \frac{di_{L2}}{dt} = V_{C2} - E - V_C \quad (7)$$

$$L \frac{di_L}{dt} = (V_{C2} - E) - V_C \quad (8)$$

$$C_1 \frac{dV_{C1}}{dt} = i_{L2} \quad (9)$$

$$C \frac{dV_C}{dt} = i_L + (i_{L1} - i_{L2}) - \frac{V_C}{R} \quad (10)$$

In steady state condition,  $\frac{di_L}{dt} = 0$  and  $V_{C1} = V$ ,  $V_{C2} = V$  and  $V_C = V_o$

So we have,

$$V_o = \frac{DV + (1-D)(V-E)}{1-D} \quad (11)$$

The above expression represents the output voltage of the topology during charging state.

$$V_o = \frac{D_2E + D_{eff}V}{1-D_1} \quad (12)$$

The above expression represents the output voltage of the topology during discharging state.

## LOSSES AND EFFICIENCY CALCULATION FOR THREE PORT TOPOLOGY

All the values of the parameters considered below are taken from their respective data sheets.

For IGBT (FGA15N120FTD)

$$\begin{aligned} \text{Conduction losses} &= V_{CE(sat)} \times I_C + R_{ON} \times I_C^2 \\ &= 1.58 \times 15 + 0.001 \times 15^2 \\ &= 23.925W \end{aligned}$$

$$\begin{aligned} \text{Switching losses} &= (E_{ON} + E_{OFF}) f_{sw} \\ &= 0.88mJ \times 5 \times 10^3 \\ &= 4.4W \end{aligned}$$

For IGBT/Diode (H15R1203)

$$\begin{aligned} \text{Conduction losses} &= V_{CE(sat)} \times I_C + R_{ON} \times I_C^2 \\ &= 1.48 \times 15 + 0.001 \times 15^2 \\ &= 22.425W \end{aligned}$$

$$\begin{aligned} \text{Switching losses} &= (E_{ON} + E_{OFF}) f_{sw} \\ &= 0.7mJ \times 5 \times 10^3 \\ &= 3.5W \end{aligned}$$

$$\begin{aligned} \text{Total Losses} &= \text{Switching losses} + \text{Conduction losses} \\ &= 23.925 + 4.4 + 22.425 + 3.5 \\ &= 54.25 W \end{aligned}$$

$$\text{Output power} = V_o \times I_o = 194.35 W$$

$$\text{Efficiency} = \frac{\text{Output power}}{\text{Output power} + \text{Losses}} \times 100$$

$$\% \eta = 78.18.$$

## PROPOSED BI-DIRECTIONAL FOUR PORT TOPOLOGY

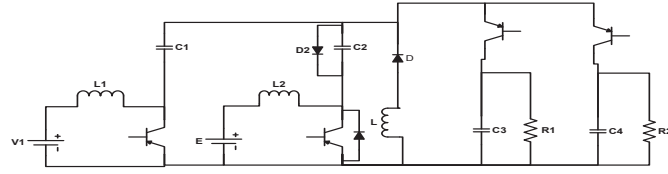


**FIGURE 7.** - Proposed Bi-directional four port SEPIC Converter

### Modes of Operation

#### *Battery Discharging ( $V < E$ )*

In this mode, both the switches  $S_1$  and  $S_2$  operate for duty cycles of  $D_1$  and  $D_2$ . Assuming the Steady state average conditions to be:

$$\frac{diL}{dt} = 0, V_{C1} = V_1, V_{C2} = E, V_{C3} = V_{01}, V_{C4} = V_{02}$$

Considering  $D_1 > D_2$  in discharging mode, the output equation can be given as:

$$V_0 = \frac{D_2 E + D_{eff} V}{1 - D_1}$$

#### *Battery Charging ( $V > E$ ):*

##### *Mode-1: $S_1$ ON, $S_2$ OFF*

In this mode switch  $S_1$  is ON and remaining all switches are OFF. The battery charges through the energy stored in the inductor  $L_2$  when switch  $S_1$  is close, the inductor  $L_1$  charges from source  $V$  and  $C_1$  discharges through  $S_1$ . The load current is supplied by individual capacitors  $C_3$  and  $C_4$ . Fig.7 shows the proposed bi-directional four port SEPIC Converter. Fig.8 shows the mode 1 operation of the converter.

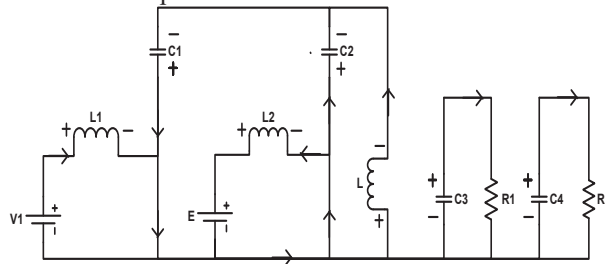


**FIGURE 8.** Mode-1:  $S_1$  ON,  $S_2$  OFF

##### *Mode-2: $S_1$ OFF, $S_2$ OFF*

In this mode of operation, all the switches are OFF because the battery has to charge. The capacitor  $C_1$  charges from the source voltage  $V$  and  $C_2$  discharges through the inductor  $L_2$  and battery which charges the inductor  $L_2$  and the battery. The load is maintained by the output capacitors. Fig.9 shows the mode 2 operation of converter.



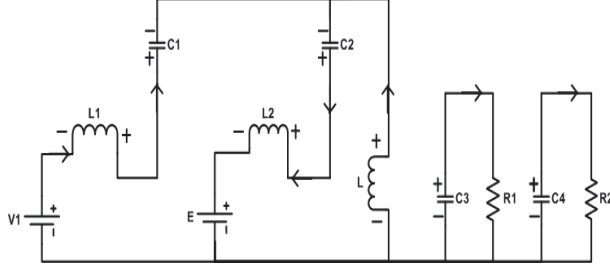


FIGURE 9. - Mode-2: S1 OFF, S2 OFF

### Steady State Analysis of Four Port Topology

Both the modes of operations are considered to be in CCM. The steady state equations of each mode are given below:

*Mode-1: S<sub>1</sub> ON, S<sub>2</sub> OFF*

$$L_1 \frac{di_{L1}}{dt} = V \quad (13)$$

$$L_2 \frac{di_{L2}}{dt} = -E \quad (14)$$

$$L \frac{di_L}{dt} = V_{C1} \quad (15)$$

$$C_1 \frac{dV_{C1}}{dt} = C_2 \frac{dV_{C2}}{dt} + i_L \quad (16)$$

$$C_3 \frac{dV_{C3}}{dt} = -\frac{V_{C3}}{R_1} \quad (17)$$

$$C_4 \frac{dV_{C4}}{dt} = -\frac{V_{C4}}{R_2} \quad (18)$$

*Mode-2: S<sub>1</sub> OFF, S<sub>2</sub> OFF*

$$L_1 \frac{di_{L1}}{dt} = V - V_{C1} - V_{C3} \quad (19)$$

$$L_1 \frac{di_{L1}}{dt} = V - V_{C1} - V_{C4} \quad (20)$$

$$L_2 \frac{di_{L2}}{dt} = V_{C2} - E - V_{C3} \quad (21)$$

$$L_2 \frac{di_{L2}}{dt} = V_{C2} - E - V_{C4} \quad (22)$$

$$L \frac{di_L}{dt} = (V_{C2} - E) - V_{C3} \quad (23)$$

$$L \frac{di_L}{dt} = (V_{C2} - E) - V_{C4} \quad (24)$$

Combining all the equations with their respective duty cycle the steady state equations of the four port topology can be written as follows:

$$L_1 \frac{di_{L1}}{dt} = D_1 V + (1 - D_1)(V - V_{C1} - V_{C3} - V_{C4}) \quad (25)$$

$$L_2 \frac{di_{L2}}{dt} = -D_1 E + (1 - D_1)(V_{C2} - E - V_{C3} - V_{C4}) \quad (26)$$

$$L \frac{di_L}{dt} = D_1 V_{C1} + (1 - D_1)((V_{C2} - E) - V_{C3} - V_{C4}) \quad (27)$$

$$C_3 \frac{dV_{C3}}{dt} = -\frac{V_{C3}D_1}{R_1} \quad (28)$$

$$C_4 \frac{dV_{C4}}{dt} = -\frac{V_{C4}D_1}{R_2} \quad (29)$$

In steady state condition,  $\frac{di_L}{dt} = 0$  and  $V_{C1} = V_{C2} = V$  and  $V_{C3} = V_{C4} = V_O$

So the output voltage expression will be

$$V_O = \frac{D_1V + (1-D_1)(V-E)}{1-D_1} \quad (30)$$

### Reverse Power Flow from Load to Source

*Mode-1: S3 OFF, S4 ON*

In this case the switch S4 is ON and remaining all switches are OFF. It is assuming that the back emf is greater than battery voltage then the power will flow from load to source through the path  $E_b, S4, D_2, L_2$  and charges the battery E. In this case some anti parallel diodes has taken in order to divert the path of energy flow which makes capacitors as open circuit.

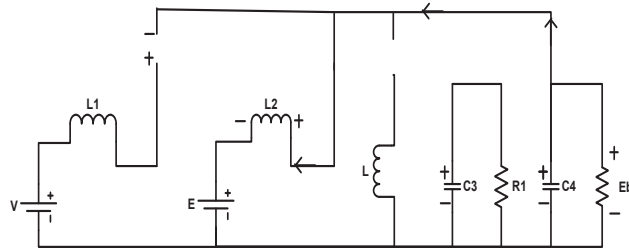


FIGURE 10.- Mode-1: S3 OFF, S4 ON

*Mode-2: S4 and S3 OFF*

During this mode all switches are OFF. The stored energy in  $L_2$  freewheels and follows a path  $L_2, E$ , anti-parallel diode of  $S_2$  and  $L_2$  thus charging the battery.

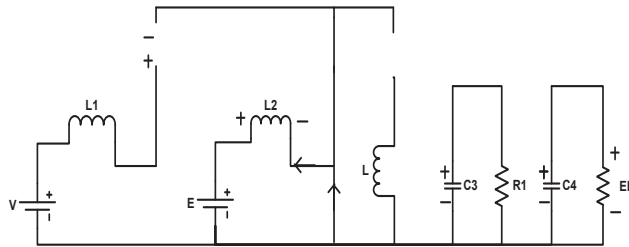


FIGURE 11. - Mode-2: S3 OFF, S4 OFF

### Small Ripple Approximation

Following the individual mode equations, the expressions of  $L_1, L_2, L, C_1, C_2, C_3$  and  $C_4$  with respect to current and voltage ripples is given below:

$$L_1 = \frac{VD_1}{f\Delta I_{L1}} \quad (31)$$

$$L_2 = \frac{ED_2}{f\Delta I_{L2}} \quad (32)$$

$$L = \frac{V_{C3}D_3}{f\Delta I_L} \quad (33)$$

$$C_1 = \frac{I_{L1}(1-D_1)}{f\Delta V_{C1}} \quad (34)$$

$$C_2 = \frac{I_{L2}(D_1+D_4)}{f\Delta V_{C2}} \quad (35)$$

$$C_3 = \frac{V_{C3}(D_2+D_D)}{fR\Delta V_{C3}} \quad (36)$$

$$C_4 = \frac{V_{C4}D_2}{fR\Delta V_{C4}} \quad (37)$$

Using the above formula we can calculate the values of inductor and capacitor.

### Losses and Efficiency of Four Port Topology

All the values of the parameters considered below are taken from their respective data sheets.

For IGBT (FGA15N120FTD)

$$\begin{aligned} \text{Conduction losses} &= V_{CE(sat)} \times I_C + R_{ON} \times I_C^2 \\ &= 1.58 \times 15 + 0.001 \times 15^2 \\ &= 23.925W \end{aligned}$$

$$\begin{aligned} \text{Switching losses} &= (E_{ON}+E_{OFF})f_{sw} \\ &= 0.88\text{mJ} \times 5 \times 10^3 \\ &= 4.4W \end{aligned}$$

For IGBT/Diode (H15R1203)

$$\begin{aligned} \text{Conduction losses} &= V_{CE(sat)} \times I_C + R_{ON} \times I_C^2 \\ &= 1.48 \times 15 + 0.001 \times 15^2 \\ &= 22.425W \end{aligned}$$

$$\begin{aligned} \text{Switching losses} &= (E_{ON}+E_{OFF}) f_{sw} \\ &= 0.7\text{mJ} \times 5 \times 10^3 \\ &= 3.5W \end{aligned}$$

$$\begin{aligned} \text{Total Losses} &= \text{Switching losses} + \text{Conduction losses} \\ &= 23.925 + 4.4 + 22.425 + 3.5 \\ &= 54.25 W \end{aligned}$$

$$\text{Output power} = V_o \times I_o = 255 W$$

$$\begin{aligned} \text{Efficiency} &= \frac{\text{Output power}}{\text{Output power} + \text{Losses}} \times 100 \\ &= \frac{255}{309.25} \times 100 \end{aligned}$$

$$\% \eta = 82.46$$

## RESULTS AND DISCUSSIONS

### Simulink Model for Three Port Topology

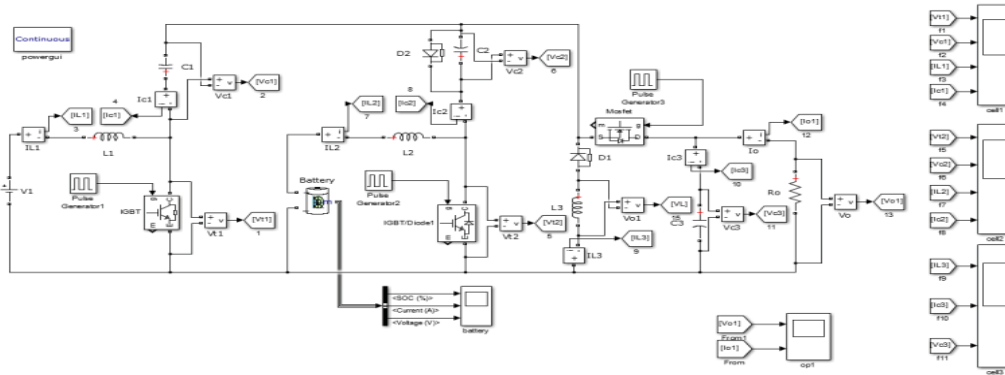


FIGURE 12 - Simulink Model for bi-directional three port topology

### Analysis of Waveforms of three Port Topology

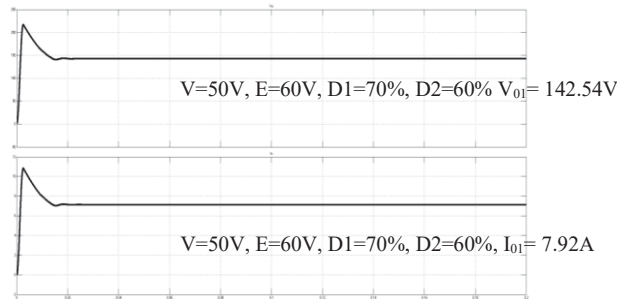


FIGURE 13.- Output voltage and current waveforms of topology (discharging)

In the proposed three port topology the values of sources  $V$  and  $E$  are given as  $50\text{ V}$  and  $60\text{ V}$  respectively during discharging mode. During discharging mode we are considering  $D1 > D2$  so the switches 1 and 2 are operated with a duty cycle of  $70\%$  and  $60\%$  respectively. The output voltage obtained is  $142.54\text{ V}$  and output current is  $7.92\text{ A}$  as shown in figure 13.

The simulation is done for different values of  $V$  and  $E$  with duty cycles  $D1$  and  $D2$  to compare simulated values and the calculated values as shown in Table 1.

**TABLE 1.** Actual and calculated output voltage of three port topology for different set of supplies with D2 constant (Discharging)

V	E	D1	D2	V <sub>o</sub> (sim)	V <sub>o</sub> (cal)
10	15	85	60	66.5	76.6
15	20	80	60	71	75
30	35	75	60	100.5	102
40	50	70	60	114.5	113.3
45	55	65	60	103.5	100.7

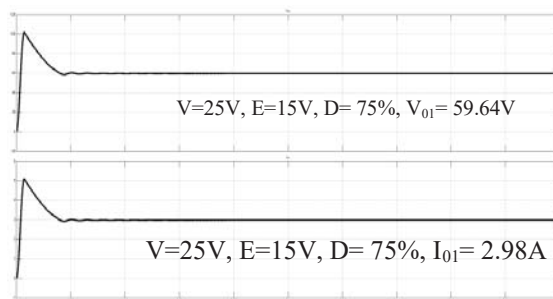


**FIGURE 14.-** Output voltage and current waveforms of three port topology (Charging)

In the proposed three port topology the values of sources V and E are given as 25 V and 15 V respectively during charging mode. During charging mode we are considering  $D1 < D2$  so the switch 1 is operated with a duty cycle of 75%. Here in the charging mode only switch 1 operates so only D1 is varied. The output voltage obtained is 59.64 V and output current is 2.98 A as shown in figure 14. The simulation is done for different values of V and E with duty cycle D to compare simulated values and the calculated values as shown in Table 5.2. The current and voltages through the inductors and capacitors on the source and the load side are shown in figure 15.

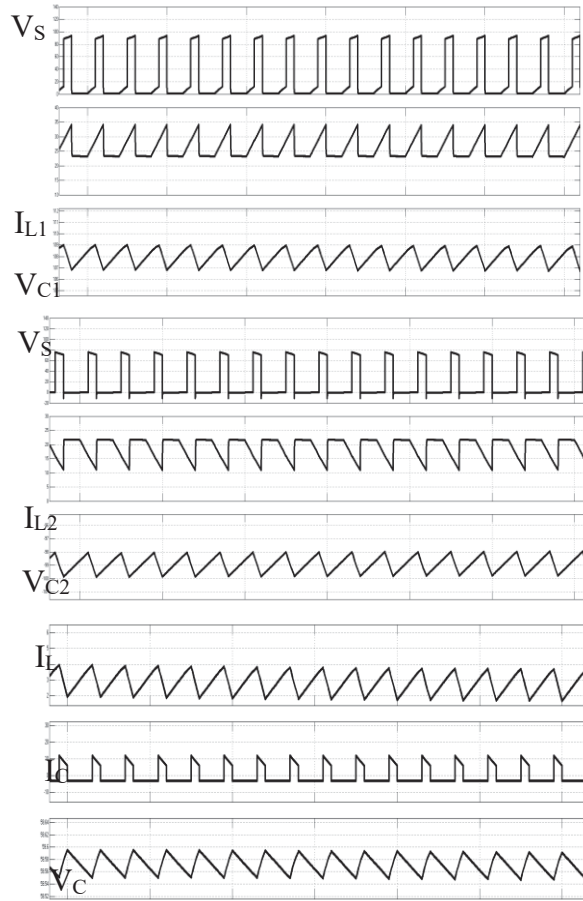


FIGURE 15.- Waveforms of voltage and current components in PVSC1, PVSC2 and PVLC (Charging)

TABLE 2. Actual and estimated output voltage of three port topology for different set of supplies (Charging)

V	E	D	V <sub>o</sub> (sim)	V <sub>o</sub> (est)
15	10	85	103	90
20	15	80	93	85
35	30	75	110	110
50	40	70	132	126.67

### 5.3 Simulink Model for Four Port Topology

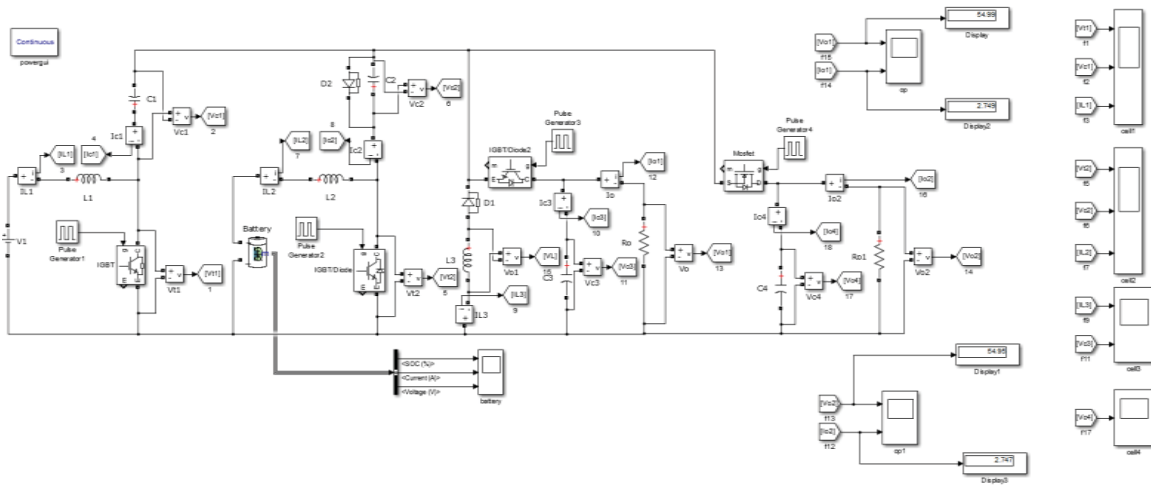


FIGURE 16. - Simulink Model for bi-directional four port topology

### 5.4 Analysis of Waveforms of four Port Topology

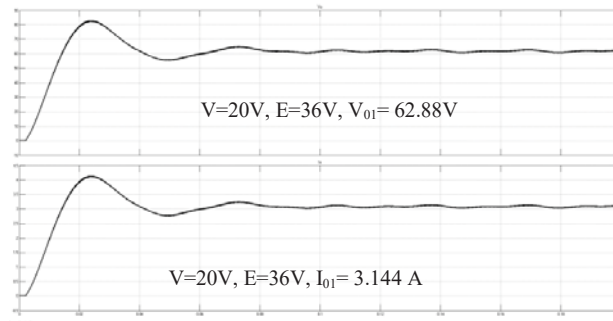


FIGURE 17.- Output voltage and current waveform of topology (Discharging)

In the proposed three port topology the values of sources  $V$  and  $E$  are given as 20 V and 36 V respectively during discharging mode. During discharging mode we are considering  $D1 > D2$  so the switches 1 and 2 are operated with a duty cycle of 65% and 50% respectively. The output voltage obtained is 62.88 V and output current is 3.14 A.

The simulation is done for different values of  $V$  and  $E$  with duty cycles  $D1$  and  $D2$  to compare simulated values and the calculated values.

TABLE 3. Actual and estimated output voltage of four port topology for different set of supplies (Discharging)

V	E	D1	D2	Vo(sim)	Vo(est)
8	12	85	50	57.5	58.6
10	12	80	50	44.6	45
16	24	75	50	64.8	64
20	36	65	50	62.8	60

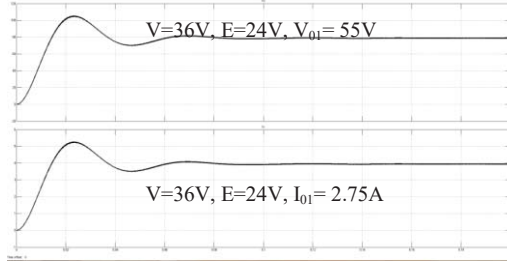


**FIGURE 18.-** Output voltage and current waveforms of four port topology (Charging)

In the proposed three port topology the values of sources  $V$  and  $E$  are given as 36 V and 24 V respectively during charging mode. During charging mode we are considering  $D1 < D2$  so the switch 1 is operated with a duty cycle of 52%. Here in the charging mode only switch 1 operates so only  $D1$  is varied. The output voltage obtained is 55 V and output current is 2.75 A. The simulation is done for different values of  $V$  and  $E$  with duty cycle  $D$  to compare simulated values and the calculated values. The current and voltages through the inductors and capacitors on the source and the load side are shown in Fig.19.

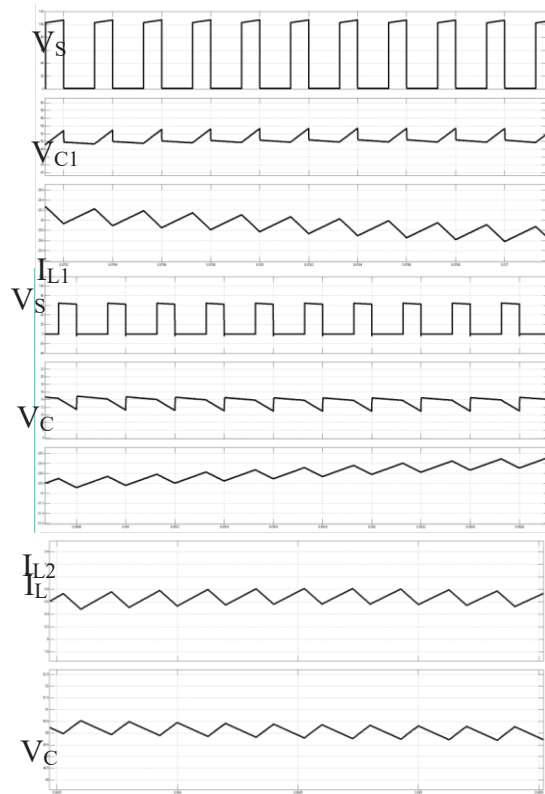


**FIGURE 19. -** Waveforms of voltage and current of components in PVSC1, PVSC2 and PVLC1 (Charging)



**TABLE 4:** Actual and estimated output voltage of four port topology for different set of supplies (Charging)

V	E	D	Vo (sim)	Vo (est)
24	12	15	16.2	16.23
42	36	30	23.86	24
36	24	52	55	51
45	30	60	82.14	82.5

## CONCLUSION

The multiport topologies for SEPIC converter were studied and three port and four port bidirectional SEPIC converters were proposed. The power management system comprises of a main source and a battery which use a single stage modified DC/DC converter to interface multiple ports. The operation of both the proposed converters was verified. The authenticity of the performance and operation of the converter was done with the help of simulations and mathematical calculations. The operating modes of the topologies were verified using simulations. The switching and conduction losses were calculated and the efficiency was determined for the three and four port bidirectional SEPIC converter.

## REFERENCES

1. Hongfei Wu, Member, IEEE, Junjun Zhang, and Yan Xing, Member, IEEE, "A Family of Multiport Buck-Boost Converters Based on DC-Link Inductors (DLIs)", *IEEE Transactions on power electronics*, Vol. 30, no. 2, February 2015, Pages: 735 - 746
2. Zubair Rehman, Ibrahim Al-Bahadly, S.C. Mukhopadhyay, "Multi-input DC-DC converters in renewable energy applications – An overview of Science Direct, *Renewable and Sustainable Energy Reviews*, Volume 41, January 2015, Pages 521–539
3. M.B. Ferrera, S.P. Litrán, E. Durán, J.M. Andújar, "A Converter for Bipolar DC Link Based on SEPIC-Cuk Combination", *IEEE Transactions on Power Electronics*, Volume: PP, Issue: 99, Year: 2015
4. Juyoung Jung and Alexis Kwasinski "A Multiple-Input SEPIC with a Bi Directional Input for Modular Distributed Generation and Energy Storage Integration", *IEEE Conference Publications on Applied Power Electronics Conference and Exposition (APEC)*, Year: 2011, Pages: 28-34
5. H. Tao, A. Kotsopoulos, J.L. Duarte and M.A.M. Hendrix, "Family of multiport bidirectional DC-DC converters", *IEE Proc.-Electr. Power Appl.*, Vol. 153, No. 3, May 2006, Pages: 451 – 458
6. Yuan-Chuan Liu and Yaow-Ming Chen, Senior Member, IEEE, "A Systematic Approach to Synthesizing Multi-Input DC-DC Converters" , *IEEE Transactions on power electronics*, Vol. 24, no. 1, January 2009, Pages: 116 – 127
7. Mario Marchesoni and Camillo Vacca, "New DC-DC Converter for Energy Storage System Interfacing in Fuel Cell Hybrid Electric Vehicles", *IEEE Transactions on power electronics*, Volume: 22, Issue: 1, Year: 2007, Pages: 301 – 308
8. Y. Chen, P. Zhang, X. Zou, and Y. Kang, "Dynamical modeling of the non-isolated single-inductor three-port converter," *Conf. Proc. - IEEE Appl. Power Electron. Conf. Expo. - APEC*, no. 2012, pp. 2067–2073, 2014.
9. J. Zhao, H. H. C. Iu, T. Fernando, L. An, and D. Dah-Chuan Lu, "Design of a non-isolated single-switch three-port DC-DC converter for standalone PV-battery power system," *Proc. - IEEE Int. Symp. Circuits Syst.*, vol. 2015-July, pp. 2493–2496, 2015.
10. S. Lu, K. A. Corzine, and M. Ferdowsi, "An unique ultracapacitor direct integration scheme in multilevel motor drives for large vehicle propulsion," *Conf. Rec. - IAS Annu. Meet. (IEEE Ind. Appl. Soc.)*, vol. 5, no. 4, pp. 2419–2426, 2006.
11. S. Lu, K. A. Corzine, and M. Ferdowsi, "An unique ultracapacitor direct integration scheme in multilevel motor drives for large vehicle propulsion," *Conf. Rec. - IAS Annu. Meet. (IEEE Ind. Appl. Soc.)*, vol. 5, no. 4, pp. 2419–2426, 2006.

12. L. Solero, F. Caricchi, F. Crescimbeni, O. Honorati, and F. Mezzetti, "Performance of A 10 kW power electronic interface for combined wind/PV isolated generating systems", PESC Rec. - IEEE Annu. Power Electron. Spec. Conf., vol. 2, pp. 1027–1032, 1996.
13. N. D. Benavides and P. L. Chapman, "Power budgeting of a multiple-input buck-boost converter," [IEEE Trans. Power Electron.](#), vol. 20, no. 6, pp. 1303–1309, 2005.
14. H. Matsuo, W. Lin, F. Kurokawa, T. Shigemizu, and N. Watanabe, "Characteristics of the multiple-input dc-dc converter," [IEEE Trans. Ind. Electron.](#), vol. 51, no. 3, pp. 625–631, 2004.
15. H. Tao, A. Kotsopoulos, J. L. Duarte, and M. A. M. Hendrix, "Family of multiport bidirectional DC – DC converters," pp. 451–458.
16. Y. Li, X. Ruan, S. Member, D. Yang, F. Liu, and C. K. Tse, "Synthesis of Multiple-Input DC / DC Converters," vol. 25, no. 9, pp. 2372–2385, 2010.
17. P. Yang, C. K. Tse, J. Xu, and G. Zhou, "Synthesis and Analysis of Double-Input Single-Output DC/DC Converters," [IEEE Trans. Ind. Electron.](#), vol. 62, no. 10, pp. 6284–6295, 2015.